Journal of Chromatography, 504 (1990) 1–19
Elsevier Science Publishers B.V., Amsterdam — Printed in The Netherlands

CHROM. 22 178

Variance contributions to band spread in capillary zone electrophoresis

HARLAN K. JONES, NHUNG T. NGUYEN and RICHARD D. SMITH*
Chemical Methods and Separations Group, Chemical Sciences Department, Pacific Northwest Laboratory, Richland, WA 99352 (U.S.A.)
(First received July 4th, 1989; revised manuscript received November 22nd, 1989)

SUMMARY

A peak variance method is described and used to determine contributions to band spread in capillary zone electrophoresis (CZE) for model systems consisting of amino acids, peptides and proteins. A theoretical and experimental approach is proposed for isolating time-independent contributions to band spread from the time-dependent contributions to band spread in CZE. The significant time-independent contributions to CZE band spread include injection and detection, while important time-dependent contributions to band spread in CZE are due to molecular diffusion, Joule heating and deviation from ideal electroosmotic plug flow. The contribution of diffusion to band spread in CZE is experimentally determined by using a new approach involving multiple passes of the sample band past the detector, allowing measurement of the total variance of a sample band at periodically increasing residence times in the CZE column. Molecular diffusion is confirmed to be the major contributor to band spread under optimized CZE conditions. The experimental values for diffusion coefficients obtained in studies (without an externally applied electric field) are subsequently used to isolate the more subtle contributions to band spread which include Joule heating and the nature of electroosmotic (*i.e.*, flow deviation from plug). Important time-independent contributions, *i.e.*, injection, detection and voltage "on–off" switching are isolated for several analytes and compared to their total experimentally determined time-independent variance.

INTRODUCTION

Capillary zone electrophoresis (CZE) has been shown to be a fast, efficient separation method for mixtures of amino acids[1,2], polypeptides[3], proteins[4–6], bases, nucleosides and oligonucleotides[7], catechols[8] and a wide range of other biologically important molecules. Martin *et al.*[9] have studied some of the factors contributing to the loss of separation efficiency in CZE which include molecular diffusion, the nature of the fluid, effects due to flow in capillaries (*i.e.*, specifically the flow profile, deviation from plug flow), heating effects, injection volume, detection volume and sample

0021-9673/90/$03.50

specific contributions (*i.e.*, concentration effects and adsorption on capillary surfaces). Coxon and Binder[10] have previously addressed the problem of the radial temperature distribution for isotachophoresis in columns of circular cross-section. Martin and Guiochon[11] have studied longitudinal dispersion in liquid chromatography for the case of electroosmotic pumping. Most recently, Foret *et al.*[12] have described some of the dispersive processes relating to CZE separation efficiency, and Grushka *et al.*[13], have examined temperature gradients in CZE for capillary columns of varying diameters. Of considerable interest are non-ideal operating conditions, where compromises to sample size and electric field gradient may be necessary to allow collection, sample fractionation, enhanced sensitivity for detection, or greater separation speed.

Most workers in the area of CZE agree that the longitudinal contribution of molecular diffusion is the predominant contribution to the broadening of the solute band under "ideal" conditions. However, it has also been observed that Joule heating and deviation from ideal electroosmotic plug flow (resulting from additional effects due to heating, and other contributions due to inadvertent laminar flow) may also contribute substantially to loss of CZE separation efficiency since optimum CZE results are defined only by the relative rates of electrophoretic migration and molecular diffusion. The molecular diffusion coefficient is also an important physical property for molecules of biological importance, *i.e.*, proteins and smaller polypeptides. When combined with sedimentation-rate measurements, the diffusion coefficient can yield accurate molecular weight values for proteins[14]. More importantly, the ability to isolate the solute band broadening contribution due to molecular diffusion is the first step toward isolating other significant band broadening factors contributing to the loss of separation efficiency in CZE (*e.g.*, heating effects and deviations from "ideal" plug-flow). Our goal in this work is to first experimentally determine the contribution of diffusion to band spread in CZE, and to use this as a basis for attempting to experimentally isolate the other (more subtle) contributions. One aspect of our approach is to attempt to separate additional contributions (due directly or indirectly to heating) from any due inherently to electroosmotic flow.

The peak variance method used in this study for determining aqueous diffusion coefficients is based on a method first introduced by Giddings and Seager[15], and later modified by Knox and McLaren[16] for rapid determination of gaseous diffusion coefficients. The method was later extended to dense gases by Balenovic *et al.*[17], small solutes in liquid systems by Grushka and Kikta[18], and macromolecules in aqueous liquids by Walters *et al.*[19]. The CZE experiment provides a uniquely useful method for such studies. In contrast to the earlier studies which measured solute band spread after a single pass through the detector, the electromigration process allows one to manipulate the direction of analyte motion by reversing the polarity of the electric field, while having a nearly negligible effect on peak variance. This technique provides a simple means for moving the solute band back and forth, many times if desired, past the detector. This study also complements other recent experimental studies which have investigated various factors governing separation efficiency for CZE[20–22]. In this work we show that those CZE methods allow rapid and accurate measurement of diffusion coefficients, as well as isolation of variance contributions due to injection. We will also show that contributions due to heating effects and deviations from plug flow are largely interdependent and less easily resolved experimentally, and will suggest methods to determine their relative importance.

THEORY

Separation efficiency in CZE is most often measured in numbers of theoretical plates (N)[1,23]. Less often one will encounter plate height in discussions of how efficient one separation is from another[24]. In this work the peak variance, which is the link between plate height and number of theoretical plates, is the basic tool used for examining the important efficiency loss factors in CZE.

We have selected the total variance of the solute band as the starting point for isolation and determination of efficiency loss factors in CZE. By using the total variance of the solute band, which ideally assumes a gaussian distribution, we can say that all those processes which contribute to the total breadth of the solute band can be sunmed in terms of their individual variances as shown in the following expression:

$$\sigma^2 = \sigma_A^2 + \sigma_B^2 + \sigma_C^2 + \ldots \quad (1)$$

In this model, we have taken the total variance of the solute band and divided it into two categories, a constant or time-independent variance (due to discrete events during the separation), and a time-dependent variance, which varies with the residence time of the solute in the CZE column until reaching the detector. Table I lists the efficiency loss factors for CZE. The constant factors include injection volume, detection volume, and voltage switching (*i.e.* effects arising from turning the high voltage "on" or "off", which may be attributed primarily to initiation or cessation of electroosmotic flow). The importance of voltage switching to the experimental procedure will be discussed later in this paper. Time-dependent factors which appear to contribute significantly to the broadening of a solute band include longitudinal molecular diffusion, heating and deviation of the electroosmotic flow profile from idealized plug flow. The total variance in eqn. 1 can be expressed in terms of these contributions by

$$\sigma^2 = \sigma_a^2 + \sigma_b^2(t) \quad (2)$$

where σ_a^2 is the time-independent or constant variance and $\sigma_b^2(t)$ is the time-dependent variance contribution.

Detection and injection are considered to be the major components of the constant part of the total variance. Sternberg[25] has derived second moment or

TABLE I

TIME-INDEPENDENT AND TIME-DEPENDENT CZE EFFICIENCY LOSS FACTORS

Time-independent contributions to variance (σ_a^2)
Injection
Detection
Voltage switching (high voltage "on" or "off")
Time-dependent contributions to variance (σ_b^2)
Molecular diffusion
Joule heating
Flow profile (deviation from plug flow)
Sample specific contributions (local concentration effects and adsorption)

variance expressions for detection and injection. The variance contribution for a finite detector path length is

$$\sigma_{\text{det}}^2 = l_i^2/12 \tag{3}$$

where l_i is the path length of the detector cell. Since CZE detection generally occurs "on column" the detection process itself does not contribute to variance except in terms of the length (in the case of this study) of capillary corresponding to the detector cell volume. The assumption most workers make regarding the shape of the electroosmotic injection profile is that it can be approximated by a sufficiently narrow band which can gradually relax (under ideal conditions) to a gaussian shaped peak longitudinally[20,26]. This is, of course, an approximation since all the factors which contribute to variance during separation can contribute to injection when electromigration is used, as in this study. However, such contributions to variances can almost always be neglected; as an example, a recent study by Rose and Jorgenson[27] comparing electromigration and hydrostatic injection showed no significant differences in the measured efficiencies. For a plug sample injection profile, the contribution to variance is identical to that for detection and is given by

$$\sigma_{\text{inj}}^2 = l_j^2/12 \tag{4}$$

where l_j is sample injection migration distance.

The electromigration injection process in CZE is the combination of two functions. The injection process begins with the sample input function which carries with it the initial sample band width[25]. The electromigration injection plug profile is convoluted onto that input function during injection. In contrast to most chromatographic injection processes, the CZE input function and electromigration injection process occur simultaneously. The volume of the injection band for electromigration can be accurately approximated (for a specific analyte) given the elctroosmotic flow-rate, the analyte's electrophoretic mobility, sample buffer, injection time and voltage. However, the importance of other contributions leading to dispersion during injection may be dependent upon design of the spcific apparatus and procedures, and remain undetermined.

There are certain sample specific time-dependent contributions to CZE band broadening which include adsorption effects and local electric field effects due to excessive sample concentrations, which are much more complex and beyond the scope of the present work. Such effects are most significant in the early stages of the separation, immediately following injection. Fortunately, experimental conditions can be adjusted to minimize such specific contributions; we believe the conditions chosen for this work allow their effects to be neglected.

A requirement in our present study is isolating and determining the magnitude of the contribution due to longitudinal molecular diffusion as it relates to the total variance of the CZE solute band. The Einstein equation[28] relates variance due to molecular diffusion to the molecular diffusion coefficient D_m

$$\sigma^2 = 2D_m t \tag{5}$$

(where t is time in s and D_m has units of cm^2/s). Measurement of the variance due to molecular diffusion is ideally accomplished in the absence of Joule heating and, less generally, electroosmotic flow, both of which are inherent to CZE (although, in specific circumstances these effects *may* be made negligible—it is unclear at what point this is accomplished). Both heating and electroosmotic flow are induced by applying an electric field gradient across the length of the fused-silica glass capillary column, so such measurements would ideally be obtained in the absence of the applied field.

Our method is similar to Knox and McLaren's[16] gas chromatographic method. During the experiment, the applied potential is turned off, which stops electroosmotic flow, and then the analyte band is allowed to spread by diffusion only. Jorgenson and co-workers[20,26] have previously used a variation of Knox's method for measurement of molecular diffusion coefficients. A difficulty encountered in this approach is that one must assume or calculate contributions from detection, injection, and interruption of both electrophoretic migration and electroosmotic flow, or to choose conditions such that (one hopes) such contributions are negligible. A dual-detector approach like the one employed by Evans and McGuffin[29] for the elimination of extra column contributions to chromatographic peak variance would prove useful for the analysis of the CZE time-independent variance contributions, but would still require a "field on" condition for the measurement of diffusion coefficients. Rather than make one measurement of the solute band during an experiment or flow the analyte between two detectors, our method allows the analyte to diffuse freely during several "field off" time periods and diffusion is determined in a straightforward manner from the contribution to variance for two (or more) different measurements of the peak. The diffusion can occur in conjunction with normal CZE conditions (*i.e.*, field on) or with the field off, to obtain accurate measurements of diffusion coefficients. At the end of each free diffusion period the electroosmotic flow is reversed and the sample is moved immediately past the detector. Electroosmotic flow is discontinued immediately following detection of the solute band. At each pass, the peak width at half-height is measured which is converted to total peak variance by the following series of expressions which are related to column efficiency or number of theoretical plates N[30],

$$N = l_k^2/\sigma^2 \tag{6}$$

where l_k is the distance from injection to detector. The following expression relates peak width at half-height to N[30].

$$N = 5.545\ (l_k^2/w_{1/2}^2) \tag{7}$$

By combining eqns. 6 and 7, total peak variance σ^2 can be directly related to the square of $w_{1/2}$

$$\sigma^2 = w_{1/2}^2/5.545 \tag{8}$$

The peak integrator used for all experiments in this study calculates the area-to-height ratio (AR/HT) of an analyte peak in units of time which is equated to peak width at half-height. The width at half-height is used rather than width at baseline to reduce errors due to any adsorption[31]. The peak width at half-height must be

converted to column length units for peak variance. Once total peak variance is calculated, a plot of total variance *versus* column residence time is determined. According to eqn. 2, constant contributions to peak variance are found in the intercept σ_a^2 and the time-dependent variance contributions are contained in the slope. In our studies (where the high voltage is off except for the brief period required to move the band past the detector at relatively modest field strengths), we show that the time-dependent variance is due only to longitudinal molecular diffusion. We demonstrate that all other contributions may be neglected for diffusion rates typical of solutes in normal liquids. By applying the Einstein eqn. 5 to the slope of the variance *versus* time plot, one directly calculates the molecular diffusion coefficient D_m. Other voltage switching experiments have been done, which yield a slope containing the variance due to diffusion plus other significant contributions to the time-dependent variance. By subtracting the variance due to diffusion from the total time-dependent variance, one can begin to investigate the other factors contributing to the loss of separation efficiency in CZE.

EXPERIMENTAL

Apparatus

The apparatus used for all electrophoresis experiments was similar in design to that described by Jorgenson and Lukacs[1]. Fused-silica capillaries with inner diameter of 100 μm were obtained from Polymicro Technologies (Phoenix, AZ, U.S.A.), and used without any further treatment. The capillaries were all 150 cm in length and in all cases filled with 0.01 *M* phosphate buffer which was adjusted to pH 8.3. A Glassman High Voltage (Whitehouse Station, NJ, U.S.A.) Model LG60P2.5 0–60 kV d.c. power supply delivered the applied potential. The high-voltage lead is contained within a plastic insulating box equipped with electrical interlocks protecting the operator from the high-voltage region. Strips of platinum foil were used as electrodes. On-column UV detection was carried out by using a modified ISCO V^4 variable-wavelength high-performance liquid chromatography (HPLC) detector (Lincoln, NE, U.S.A.) at 215 or 280 nm. On-column fluorescence detection was carried out by using a McPherson FL-749 spectrofluorometer, Division of Schoeffel International (Acton, MA, U.S.A.). A 150 W Xenon short-arc lamp was used as the excitation source; fluorescence light was collected at 90° to the excitation beam through a 440-nm glass cut-off filter. Output signals from both absorbance and fluorescence detectors were connected to a 3390A Reporting Integrator, Hewlett Packard (Avondale, PA, U.S.A.). The window of the on-column detector cell was created by burning a small section of the polyimide coating off at the mid-point (75 cm) of the 150-cm capillary column. The on-column fluorescence cell length was 0.107 cm, and the on-column UV–VIS detector cell length was 0.104 cm.

Procedure

Sample was introduced by electromigration at the high-voltage end of the capillary column. Samples were prepared at the given concentration in the buffer used for CZE separation. For all cases except horse heart myoglobin, injection was done at 15 kV applied potential for 3 s with a current of 5.9 μA. In the case of myoglobin, injection was done at 10 kV applied potential for 5 s with a current of 4.1 μA. The

TABLE II

MOLECULAR WEIGHTS AND CONCENTRATIONS OF AMINO ACIDS, POLYPEPTIDES AND PROTEINS IN THIS STUDY

Sample	*Molecular weight*	*Sample concentration*
2-Naphthol	144	$5.80 \cdot 10^{-4}$
Dns-Ala	421	$1.92 \cdot 10^{-4}$
Dns-Ile	463	$1.88 \cdot 10^{-4}$
FL-methionine enkephalinamide[a]	868	$2.88 \cdot 10^{-5}$
FL-vacotocin[a]	2450	$5.10 \cdot 10^{-6}$
FL-insulin[a]	8220	$6.00 \cdot 10^{-5}$
Horse heart myoglobin	17 500	$3.57 \cdot 10^{-5}$

[a] FL corresponds to the fluorescamine labeled polypeptides and protein.

potential applied at the beginning of each experiment was 30 kV with a current of 12.5 μA. The high voltage remained on until the sample peak was detected. Immediately following detection, the applied potential was turned off for a period of approximately 60 min. At the end of 60 min, the ends of the capillary column were interchanged (reversing the electric field after voltage is reapplied), which caused a change in the direction of the elctroosmotic flow. The 30 kV potential was reapplied for as long as it took for the sample peak to be detected and then discontinued again for another 60-min period. This procedure was repeated a number of times. Any flow in the capillary due to a difference in reservoir heights was immediately apparent by a change in the amount of time required for detection when voltage was reapplied (ideally the time between detection of the peak maximum and turning the voltage off is precisely the same as the time between reapplying voltage and detection). A modification of the above experiment was done by keeping the voltage on throughout the entire experiment except during the 30-s periods when the column ends were interchanged to reverse the direction of electroosmotic flow. 2-Naphthol, dansyl-L-alanine (Dns-Ala) and dansyl-L-isoleucine (Dns-Ile) were studied by using the modified procedure at the following applied potentials: 30, 25, 20, 15, 10 and 5 kV.

Column maintenance

Buffer reservoirs were replenished with fresh buffer daily. The capillary column was flushed with 200 μl of fresh buffer each day before use. For separations of polypeptides and proteins the column was flushed with fresh buffer after each experiment.

Chemicals

Table II lists the amino acids, polypeptides, proteins and other molecules used in this work, their respective molecular weights and concentrations used for most studies. Fluorescamine was used to label the polypeptides and insulin for fluorescence detection. All of the polypeptides, proteins, dansylated amino acids, and fluorescamine used in this study were obtained from Sigma. Phosphate buffers were prepared from reagent-grade chemicals (NaH_2PO_4, Na_2HPO_4 and NaOH) and had an ionic strength of 0.01 *M* and a conductivity of 670 μS.

TABLE III

CONTRIBUTIONS TO THE TIME-INDEPENDENT VARIANCE

Sample	σ^2_{det} (cm^2)	σ^2_{inj} (cm^2)	$\sigma^2_{det} + \sigma^2_{inj}$ (cm^2)	σ^2_{exp} (cm^2)
2-Naphthol	0.000952	0.00608	0.00703	0.0510
Dns-Ala	0.000952	0.00396	0.00491	0.0348
Dns-Ile	0.000952	0.00378	0.00473	0.0365
FL-methionin enkephalinamide	0.000952	0.00456	0.00551	0.0190
FL-vacotocin	0.000952	0.00621	0.00716	0.0779
FL-insulin	0.000952	0.00059	0.00154	0.0268
Horse heart myoglobin	0.000906	0.00658	0.00749	0.0689

RESULTS AND DISCUSSION

The focus of this paper is measurement of the variance due to molecular diffusion, which we classify as a component of the time-dependent part of the total variance of the solute band (see Theory section). We then use these techniques to examine other contributions to variance. As a preface to the discussion of the molecular diffusion experiments, the time-independent part of the total variance requires a brief discussion.

Contributions due to injection and detection

Table III lists results for all the compounds used in the band spread study. The corresponding calculated time-independent variance values due to detection and injection and their respective sums are compared to the total experimental time-independent variance. Table IV shows the experimental contribution of voltage switching to the total time-independent variance for 2-naphthol and horse heart myoglobin. The voltage switching variance accounts for one cycle of turning the applied potential on and off.

The calculated variance due to detector path length will be the same for all molecules except horse heart myoglobin, where on-column UV absorbance detection was used. The detector variance, calculated from eqn. 3, is approximately 50 times smaller than the total experimental time-independent variance for each molecule.

The variance due to electromigration injection was calculated from eqn. 4. The

TABLE IV

VOLTAGE SWITCHING CORRECTION (σ^2_{vs}) TO THE TIME-INDEPENDENT VARIANCE

Sample	$\sigma^2_{det} + \sigma^2_{inj}$ (cm^2)	σ^2_{exp} (cm^2)	σ^2_{vs} (cm^2)	$\sigma^2_{correc.}$ (cm^2)
2-Naphthol	0.00703	0.0510	0.0012	0.0498
Horse heart myoglobin	0.00749	0.0689	0.0018	0.0671

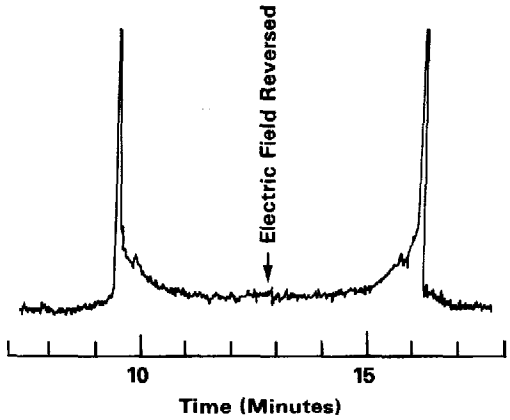

Fig. 1. Peak tailing due to poor manual electroosmotic injection, shown before and after reversing the polarity of the applied potential.

calculated variances for this mode of injection are all approximately an order of magnitude less than their respective total experimental variances. The summed variance due solely to detection and injection is approximately 7 times less than the total experimental variance for each sample molecule. While some of the difference may be due to voltage switching, the majority of the time-independent variance can be directly attributed to injection processes. An extreme case of poor manual electromigration injection is illustrated in Fig. 1. The tailing portion of the first 2-naphthol peak is the result of poor injection technique. Some experimental factors which can lead to band broadening during injection have been described by Grushka and McCormick[22]. Following reversal of the electric field, the same contribution to band spread due to injection is shown reflected as the leading portion of the 2-naphthol

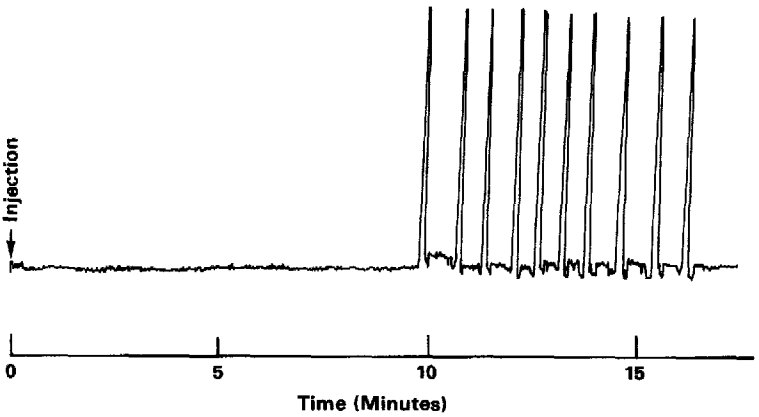

Fig. 2. Effect of reversing high-voltage polarity nine times to determine contributions to peak variance. The analyte was 2-naphthol (10^{-4} *M*), pH 8.3 phosphate buffer (10^{-2} *M*), 3-s/5-kV injection, 30 kV applied potential.

peak. Manual injection can be markedly improved by repetition and practice, and was utilized in all experiments. The important point relevant to the present study is that injection quality is verified by the initial passage through the detector at the start of each expriment, and any non-ideal effects due to injection or the early stages of electromigration are explicitly subtracted.

Contributions to peak variance from voltage switching

The voltage switching technique used in this study allows repetitive detection of sample bands during the CZE experiment by reversing the direction of electroosmotic flow. The peak width was independent of any additional delay after detection (before removing the high voltage) *i.e.*, subsequent detection did not indicate any effect of the time between between applying high voltage and peak width. These results indicate that electroosmotic flow is established very rapidly (or stopped very rapidly). In Table IV, experimental variance values for 2-naphthol and horse heart myoglobin are given for voltage switching (σ^2_{vs}). Fig. 2 shows an electropherogram illustrating the effect of voltage switching for 2-naphthol. The sample migrates through the column in response to the applied potential and passes through the detector. Following sample detection the voltage is turned off, the column ends are reversed and the voltage is turned back on (alternatively, the high-voltage polarity can be inverted). The variance due to voltage switching is assumed to be a constant for a given voltage, buffer and capillary diameter, but the contributions are cumulative and depend on the number of times the high voltage is switched off and on. Each time the voltage is switched off and on, a finite constant contribution to the variance of the sample band is added. If electromigration is the mode of injection, then such a situation applies at least once in a CZE separation. In the case of 2-naphthol, the experimental variance at experimental conditions due to one voltage off–on cycle is 0.0012 cm^2, and for horse heart myoglobin the voltage off–on variance is 0.0018 cm^2. Since these measurements neglect additional contributions to peak variance due to diffusion between measurements and any disruption due to the capillary manipulation, the values reported represent the maximum possible contribution from voltage switching. The electromigration injection procedure and its corresponding voltage off–on cycle is included in our time-independent variance contribution. In Table IV, the voltage off–on variance for 2-naphthol and horse heart myoglobin has been combined with their respective detection and injection variances and then subtracted from the total experimental time-independent variance. The time-independent variance, which has been corrected for voltage switching, is approximately 7 times greater in magnitude than the summed detection and injection variance for 2-naphthol and about 9 times the magnitude of $\sigma^2_{det+inj}$ for horse heart myoglobin. The remaining experimental time-independent variance is attributed to the injection input function discussed earlier.

The present results are also of practical interest since many situations exist where one may desire to stop or slow electromigration. For example, CZE fraction collection may require removal of high voltage for a brief period. Similarly, by dropping CZE voltage, or even stopping electromigration, the detector time constant can be increased, resulting in greater signal-to-noise or (at fixed detection time constant) often greater resolution. The present results show that the effects of such voltage changes will be small and will not, in general, significantly degrade separations.

Determination of molecular diffusion contributions to peak variance

Isolating the variance contribution due to molecular diffusion from other time-dependent broadening phenomena requires an approach which minimizes, or ideally eliminates, contributions due to Joule heating and the electroosmotic flow. The first step of our approach is the same as for a normal CZE experiment; the applied potential remains on until the sample peak is detected. Immediately following detection the power supply is turned off and the sample band is allowed to spread solely due to diffusion. The experiments included four free diffusion periods, with each free diffusion period lasting about 60 min. The variance for each peak detected in an experiment (corrected for voltage switching at each voltage on–off event) is calculated from peak width at half-height according to eqn. 8 and plotted against column residence time. The data show a linear relationship to residence time with the intercept corresponding to time-independent variance contributions and the slope directly

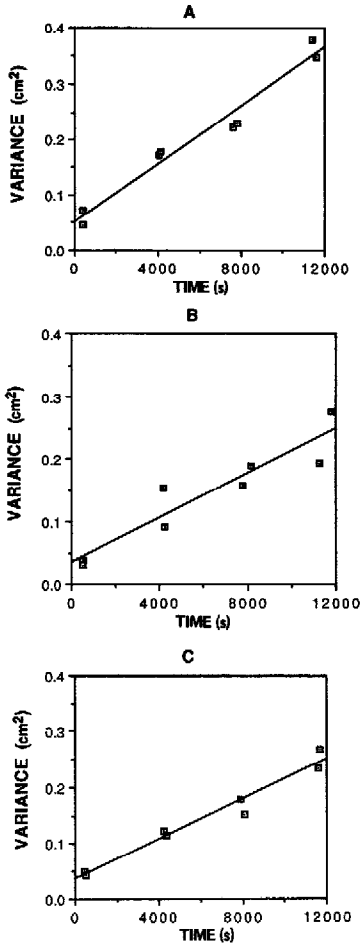

Fig. 3. Variance *versus* time plots for (A) 2-naphthol; (B) Dns-Ala; (C) Dns-Ile. Plots are used to isolate the variance contribution due to molecular diffusion.

TABLE V

MOLECULAR DIFFUSION COEFFICIENTS DETERMINED BY THE CAPILLARY ELECTROPHORESIS VARIANCE METHOD COMPARED TO VALUES DETERMINED BY OTHER METHODS

Sample	$D_m \cdot 10^6$ *by CZE variance method*[a]	$D_m \cdot 10^6$ *by other capillary electrophoresis methods*[b]	$D_m \cdot 10^6$ *by sedimentation-rate measurement*	$D_m \cdot 10^6$ *by laminar flow analysis*
2-Naphthol	13.0		12.1	
Dns-Ala	8.75	6.09		
Dns-Ile	8.77	5.37		
FL-methionine enkephalinamide	6.43			
FL-vacotocin	5.59			
FL-insulin	3.27		2.86	1.17
Horse heart myoglobin	2.06	1.15	1.13	1.03

[a] Determined without the presence of an applied electric field, at 25°C.
[b] Determined at an applied potential of 2.5 kV (ref. 20).

proportional to the molecular diffusion coefficient from eqn. 2. Fig. 3 shows a least-squares fit for three plots of total variance *versus* time for 2-naphthol, Dns-Ala and Dns-Ile. The diffusion coefficient can be calculated by applying the Einstein eqn. 5 to the slope of the line. The total variance due to molecular diffusion can then be determined for any CZE separation time.

Table V lists in order of increasing molecular weight molecular diffusion coefficients determined by the CZE variance method. Corrected molecular diffusion coefficients have been calculated for all the samples by subtracting the voltage switching variance from the uncorrected variance due to molecular diffusion. Diffusion coefficients determined by using other methods are also compared in Table V. As molecular weight increases, the molecular diffusion coefficient decreases, as expected. Our diffusion coefficients generally compare favorably with those values determined by other workers and methods, although slightly different temperatures and buffer compositions apply to each set of measurements. Somewhat surprisingly, the diffusion coefficient values determined by the present CZE variance method are slightly higher than the literature values. 2-Naphthol has a corrected diffusion coefficient (corrected for voltage switching) of $1.30 \cdot 10^{-5}$ cm^2/s compared to the literature value of $1.21 \cdot 10^{-5}$ cm^2/s, a difference of 6.9%. At the other end of the molecular weight range, horse heart myoglobin has a corrected diffusion coefficient of $2.06 \cdot 10^{-6}$ cm^2/s compared to $1.15 \cdot 10^{-6}$ cm^2/s as determined by Walbroehl and Jorgenson[20] using another capillary electrophoresis method (involving electrophoresis at low voltages where Joule heating effects should be small) and $1.13 \cdot 10^{-6}$ cm^2/s as determined by the sedimentation rate method. In the case of insulin, the percent deviation between our value and the literature value is approximately 15%, and for the dansylated amino acids the deviation is about 30%. No literature values were available for the two polypeptides. Rather than measuring peaks by AR/HT ratio which assumes a gaussian solute band distribution (and presumably valid for the symmetrical peaks generally obtained in this study), greater precision may be obtained by using

a moments analysis measurement of peak variance. The moments analysis of chromatographic peaks has been shown to yield more accurate peak variance values than the AR/HT method[31], but an evaluation of other peak measurement methods with respect to the CZE band spread study is needed prior to selecting a more accurate method. However, the ease, speed, reproducibility, and low instrumentation costs suggest that the present method has significant potential for routine measurements of diffusion coefficient. Our slightly higher values for molecular diffusion coefficients may be due to surface adsorption onto the untreated silica capillary walls, although the present methods would be expected to minimize any such effects. Surface adsorption can be best reduced by the appropriate choice of buffer pH (*i.e.*, choose a buffer pH that is above the isoelectric pH of the sample molecule, which will place a net negative charge on both the molecule and capillary wall), buffer ionic strength and sample concentration. Even when the net charge of the polypeptide or protein is the same as the capillary wall, therefore causing repulsion of the molecule from the wall, there may still be some surface adsorption due to interaction between hydrophobic sites on the molecule and the capillary wall. Sample concentration also needs to be at least two orders of magnitude less than the concentration of the buffer to avoid localized heating which could lead to measurable band spread (but not during the free diffusion period in the present study where no field is applied). Even lower molar concentrations are required for proteins which may carry numerous charges. One can sometimes minimize band spread due to surface adsorption by applying the lowest possible sample size. Since 2-naphthol, Dns-Ala and Dns-Ile were all near the upper concentration limit, band broadening due to concentration effects might be possible. By avoiding effects in the early stages of separation, the present methods should minimize such contributions. We tentatively conclude that our diffusion measurements are valid under the present experimental conditions, but additional studies are required to determine the origin of the differences obtained in comparison with other methods.

Variance contributions during CZE separations

Following determination of diffusion coefficients by the CZE variance method, the diffusion coefficient values were then used to examine the more subtle contributions of Joule heating and electroosmotic flow to sample band spread. The expriments were designed to investigate effects due to both heating and any potentially non-ideal contributions (*i.e.*, deviations from plug flow) due to the electroosmotic flow profile. The analyte migrated past the detector and was not stopped until it had almost electromigrated from the other end of the capillary. At that time the voltage was turned off and the polarity reversed. The sample was passed back and forth through the detector as in the measurements of diffusion coefficients; however, the only time the voltage was off was during 30-s periods when the ends of the column were reversed. The experiments were run at 6 different applied potentials; 30, 25, 20, 15, 10 and 5 kV. The three molecules used in the experiments were 2-naphthol, Dns-Ala and Dns-Ile. In contrast to the diffusion coefficient experiment, the voltage remains on throughout this experiment and analyte variance is due to the combined effects of diffusion, heating and electroosmotic flow.

Peak variance was measured as it was in the diffusion experiments and is given as plots of total variance *versus* time data. Fig. 4 shows electropherograms for the

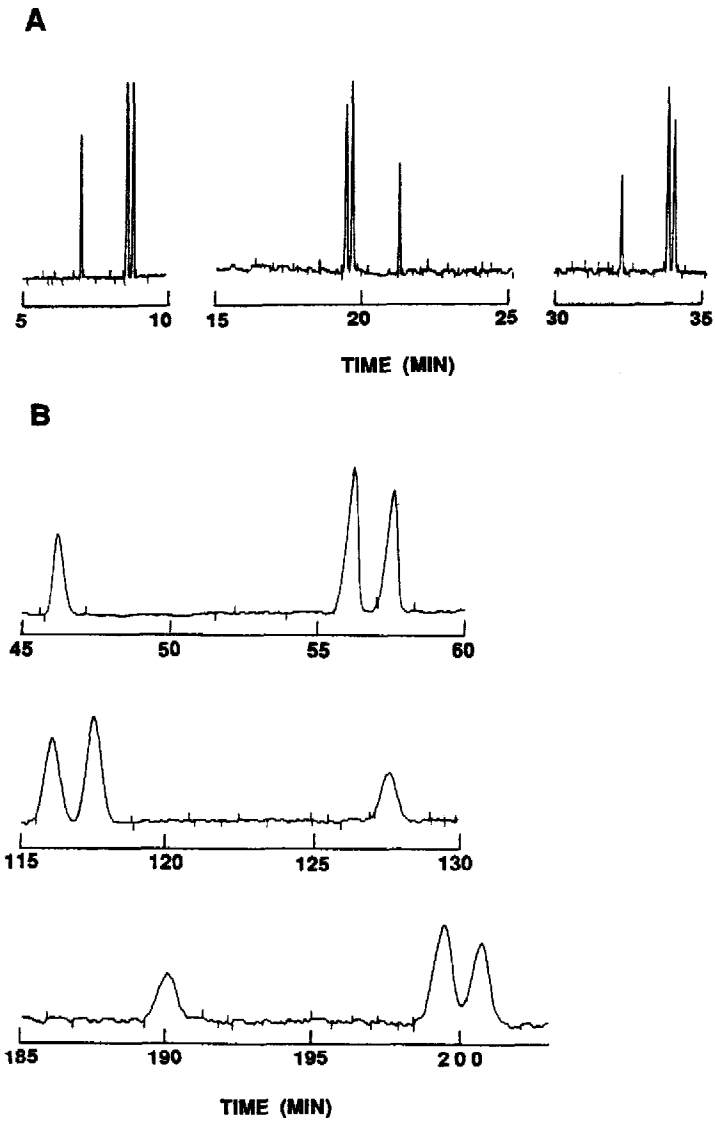

Fig. 4. Electropherograms at (A) 30 kV and at (B) 5 kV for a three-component mixture of (in order of retention times in first segment of the three segments shown) 2-naphthol, Dns-Ala and Dns-Ile. Band broadening is mainly due to molecular diffusion, heating and non-ideal flow effects.

three-component mixture for the first three measurements at 30 and 5 kV, the two extremes in applied potential. One can visually inspect the differences in band spread for each of the three components at 30 and 5 kV and observe the significant broadening of analyte peaks at the lower applied potential of 5 kV. The greater peak width obtained at 5 kV is due to slower migration through the detector, and does not effect variance measurements. Deconvolution of the relative magnitudes of the various time-dependent contributions to band spread requires a variance *versus* time plot for

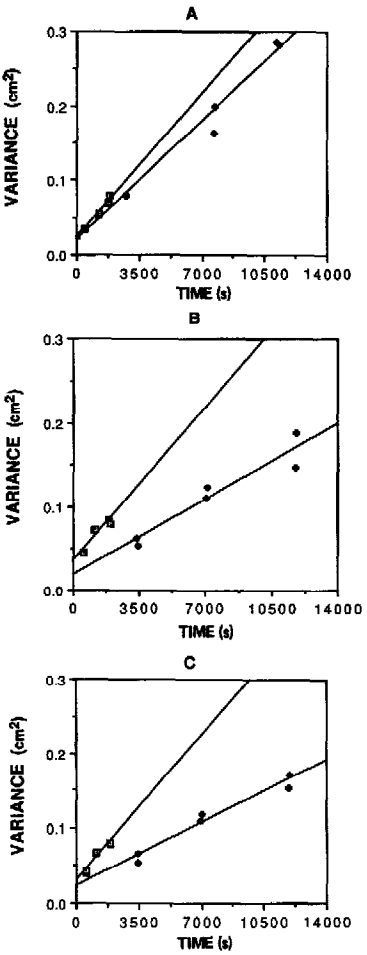

Fig. 5. CZE variable-voltage plots of total variance *versus* time for (A) 2-naphthol; (B) Dns-Ala; and (C) Dns-Ile at (□) 30 and (◆) 5 kV. These plots are generated from electropherograms similar to those shown in Fig. 4.

peaks which have undergone separations at different applied potentials. One can then isolate the time-independent contributions to band spread from the time-dependent contributions. Fig. 5 shows the plotted total variance *versus* time data for the peaks presented in Fig. 4. The time-independent contribution to peak variance is again denoted by the intercept on the variance axis. The time-independent variance includes detection, injection and voltage "on–off" contributions, the same as in the diffusion experiments. The difference between these experiments and the diffusion coefficient experiments is apparent in the slope or time-dependent variance contribution. The slope of the variance *versus* time plot contains not only variance due to molecular diffusion, but also other contributions resulting from the continuously applied potential. Joule heating and deviation from ideal plug flow are the most likely

significant contributions to time-dependent peak variance, assuming negligible surface adsorption and concentration effects.

One way to look at the combined effect of heating and non-ideal plug flow in terms of peak variance is to compare the slopes of the 30 and 5 kV experiments for 2-naphthol, a neutral molecule at pH 8.3, to the slopes of the two negatively charged amino acids Dns-Ile and Dns-Ala at the same applied potentials. Fig. 5A shows the 30 and 5 kV data plotted for 2-naphthol. The slopes of the two lines differ by approximately 16%. In the case of Dns-Ile, the slope of the 30 kV line is about 60% greater than the 5 kV slope and similarly, the 30 kV slope for Dns-Ala is 50% greater than its 5 kV slope. The neutral 2-naphthol band will not be directly influenced by *local* Joule heating (due to the presence of a higher conductivity band) since it does not carry a charge. Time-dependent band spread for 2-naphthol is therefore largely ascribed to molecular diffusion, non-ideal electroosmotic flow effects, and primary and secondary effects due to overall Joule heating of the capillary (which should be small due to the low currents utilized). Dns-Ile and Dns-Ala both carry a net negative charge and both will be influenced by local Joule heating, local changes in electric field strength (and resulting secondary effects), as well as any contribution due to deviation from plug flow and molecular diffusion. The comparison of total variance *versus* time plots for the 30 and 5 kV experiments in Fig. 5 suggests that the change in slope over the entire range of applied potentials may provide useful information regarding the isolation of ideal electroosmotic flow deviations from local effects due to Joule heating and field inhomogeneity.

Fig. 6 shows plots of slope *versus* applied potential for 2-naphthol, Dns-Ala and Dns-Ile. If disruptive effects were absent and ideal plug flow existed, the major contributor to time-dependent variance would be longitudinal molecular diffusion, and its slope would not change over the range of applied potentials. All total variance *versus* time plots would have the same slope, and slope *versus* applied potential would yield a horizontal line if molecular diffusion was the only contribution to time-dependent variance. The data shown in Figs. 5 and 6 confirm that molecular diffusion is not the only influence on time-dependent variance. Despite the scatter about the least squares fit for 2-naphthol in Fig. 6A, the data show a slight positive change in slope as voltage is increased from 5 to 30 kV, indicating other processes are contributing to the time-dependent variance. In the case of 2-naphthol, the additional effect contributing to band spread can be ascribed (with the assumption that effects of Joule heating to the buffer are minimal) to non-ideal plug flow and can be quantified over the 30 kV applied potential range in terms of cm^2/s^2-kV.

In Fig. 6B and C, Dns-Ala and Dns-Ile each show a more significant change in slope than 2-naphthol in Fig. 6A. For Dns-Ala and Dns-Ile, the change in slope over the 30 kV applied potential range provides preliminary quantitative evidence for the combined local heating and flow profile contributions to time-dependent peak variance. The total change in slope for 2-naphthol which contains these contributions is approximately $2 \cdot 10^{-7}$ cm^2/s^2-kV. The change in slope for each amino acid is about three times the change for 2-naphthol or $6 \cdot 10^{-7}$ cm^2/s^2-kV and contains the combined peak variance contributions of diffusion, non-ideal flow and Joule heating. One can readily isolate the molecular diffusion contribution from non-ideal flow in the case of 2-naphthol, but the combined effects of diffusion, Joule heating and non-ideal flow contributions to variance for Dns-Ala and Dns-Ile are not as easily separated.

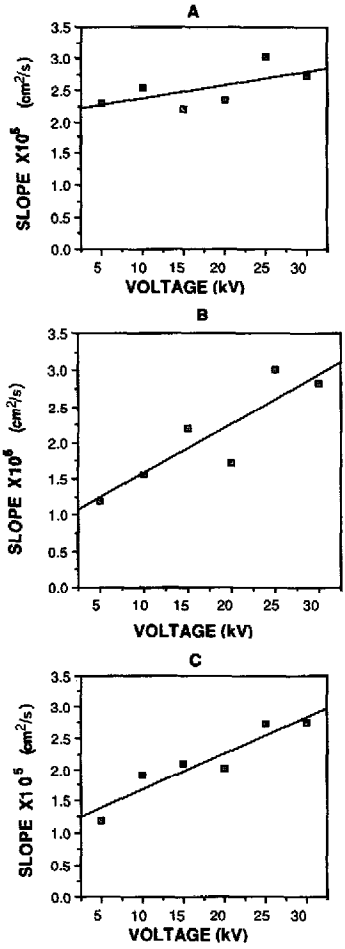

Fig. 6. CZE variable-voltage plots of slope (from variance *versus* time plots) *versus* applied potential for (A) 2-naphthol; (B) Dns-Ala; and (C) Dns-Ile. Plots are derived from a series of plots like those in Fig. 5 for the voltage range 0–30 kV, and experimentally confirm the presence of band spread due to effects other than molecular diffusion.

Subsequent studies are thus needed to isolate the contributions due to Joule heating from that due to non-ideal flow behavior.

CONCLUSIONS

Serial measurements of the total variance of a solute band during CZE separations show promise as a method for investigating the contributions to loss of efficiency. Time-independent contributions which include injection, detection and voltage switching can be calculated or determined experimentally. Injection and detection variances are often assumed to have plug flow profiles and calculated according to the equations of Sternberg[25]. Experimentally, however, injection can

result in additional variance contributions, which can be readily isolated using the methods described here. The variance due to voltage switching during separation was measured and determined to be small compared to the total time-independent peak variance. The results of these experiments indicate that effects due to voltage switching are generally negligible. This result is significant since it confirms that one can manipulate electric field strength during a separation to allow improved injection or detection (*i.e.*, slower peak passage through the detector region), or finer control of sample collection without significant degrading of the separation.

The time-dependent peak variance due to longitudinal molecular diffusion was determined experimentally for several molecules and their respective molecular diffusion coefficients were calculated from the Einstein equation. The diffusion coefficients determined by our CZE voltage switching experiments were higher than, but still compared favorably with, diffusion coefficients measured by other methods. The differences in diffusion coefficients obtained by CZE voltage switching and from other methods require further study, but the ease, quality and conceptual simplicity of the present method argues in its favor.

The CZE voltage switching method introduced in this work was extended and slightly modified for the study of Joule heating and non-ideal plug flow contributions to the time-dependent peak variance. This study was limited to three molecules: 2-naphthol, neutral at the experimental pH of 8.3, and Dns-Ile and Dns-Ala, which both carry net negative charges. In order to look at heating and flow effects, the applied potential was held constant throughout each experiment, and was turned off momentarily only to reverse the direction of electroosmotic flow.

As a result of the neutrality of 2-naphthol, both molecular diffusion and any non-ideal flow effects will contribute to its time-dependent peak variance, but not electrophoretic effects due to local heating of the solute band. It was observed that with increase of the applied potential, the slope of the peak variance *versus* time plot increased in magnitude. If only molecular diffusion was causing time-dependent variance, there should be negligible slope change over the experimental range of applied voltages since the calculated temperature increase was less than 1°C. To achieve improved quantitative values for the non-ideal flow contribution to time-dependent peak variance for 2-naphthol, the slope change from the variance *versus* time plot was plotted against applied potential. Over the 30 kV range of applied potential, the slope change increased by $6.6 \cdot 10^{-6}$ cm^2/s. Again, if only diffusion contributed to time-dependent peak variance, slope *versus* applied potential would yield a horizontal line. Our measurements show a positive increase in slope over the 30 kV range of applied potential. The increase in slope for compounds with zero electrophoretic mobility, such as neutral 2-naphthol, is the first step in isolating any non-ideal plug flow contribution to the time-dependent peak variance. Similar studies are required at a fixed voltage as a function of CZE current to determine the general contribution due to Joule heating. Similarly, the change in slope from the variance *versus* time plots of Dns-Ile and Dns-Ala was plotted against applied potential. Again, if only molecular diffusion contributed to time-dependent variance, the slope change over the range of applied potentials should be negligible for the two negatively charged dansylated amino acids. The two amino acids behaved like 2-naphthol in that they showed a positive change in slope over the 30 kV range, but the magnitude of the slope change for each amino acid was on the average a factor of 3 greater than that for

2-naphthol. The change in slope over the 30 kV applied potential range for Dns-Ala was $20 \cdot 10^{-6}$ cm^2/s and for Dns-Ile was $17 \cdot 10^{-6}$ cm^2/s.

For neutral molecules which are not directly affected by Joule heating, one can isolate the significant time-dependent band broadening factors, but for charged species one has to minimize heating effects to study non-ideal flow effects, and in turn minimize non-ideal flow effects to study the effects of Joule heating. If one makes the assumption that "non-ideal" flow effects are the same for all three analytes, then one can estimate that local Joule heating is approximately twice as significant under the experimental conditions chosen compared to any "non-ideal" flow contributions to solute band spread.

ACKNOWLEDGEMENTS

We thank the U.S. Department of Energy, Office of Health and Environmental Research, for support of this research under Contract DE-AC06-76RLO 1830. Pacific Northwest Laboratory is operated by Battelle Memorial Institute.

REFERENCES

1 J. W. Jorgenson and K. D. Lukacs, *Anal. Chem.*, 53 (1981) 1298.
2 E. Gassmann, J. E. Kuo and R. N. Zare, *Science (Washington, D.C.)*, 230 (1985) 813.
3 J. W. Jorgenson and K. D. Lukacs, *J. Chromatogr.*, 281 (1981) 209.
4 J. W. Jorgenson and K. D. Lukacs, *Science (Washington, D.C.)*, 222 (1983) 266.
5 H. H. Lauer and D. McManigill, *Anal. Chem.*, 58 (1986) 166.
6 R. M. McCormick, *Anal. Chem.*, 60 (1988) 2322.
7 A. S. Cohen, S. Terabe, J. A. Smith and B. L. Karger, *Anal. Chem.*, 59 (1987) 1021.
8 R. A. Wallingford and A. G. Ewing, *Anal. Chem.*, 60 (1988) 258.
9 M. Martin, G. Guiochon, Y. Walbroehl and J. W. Jorgenson, *Anal. Chem.*, 57 (1985) 559.
10 M. Coxon and M. J. Binder, *J. Chromatogr.*, 101 (1974) 1.
11 M. Martin and G. Guiochon, *Anal. Chem.*, 56 (1984) 614.
12 F. Foret, M. Deml and P. Boček, *J. Chromatogr.*, 452 (1988) 601.
13 E. Grushka, R. M. McCormick and J. J. Kirkland, *Anal. Chem.*, 61 (1989) 241.
14 A. L. Lehninger (Editor), *Biochemistry*, Worth Publishers, New York, 1975, Ch. 7.
15 J. C. Giddings and S. L. Seager, *J. Chem. Phys.*, 33 (1960) 1579.
16 J. H. Knox and L. McLaren, *Anal. Chem.*, 36 (1964) 1477.
17 Z. Balenovic, M. N. Myers and J. C. Giddings, *J. Chem. Phys.*, 52 (1970) 915.
18 E. Grushka and J. Kikta, *J. Phys. Chem.*, 78 (1974) 2297.
19 R. R. Walters, J. F. Graham, R. M. Moore and D. J. Anderson, *Anal. Biochem.*, 140 (1984) 190.
20 Y. Walbroehl and J. W. Jorgenson, *J. Microcolumn Sep.*, 1 (1989) 41.
21 A. E. Jones and E. Grushka, *J. Chromatogr.*, 466 (1989) 219.
22 E. Grushka and R. M. McCormick, *J. Chromatogr.*, 471 (1989) 421.
23 J. S. Green and J. W. Jorgenson, *J. High Resolut. Chromatogr. Chromatogr. Commun.*, 7 (1984) 529.
24 T. Tsuda, K. Nomura and G. Nakagawa, *J. Chromatogr.*, 248 (1982) 241.
25 J. C. Sternberg, *Adv. Chromatogr. (NY)*, 2 (1966) 205.
26 Y. Walbroehl, *Ph.D. Dissertation*, University of North Carolina, Chapel Hill, NC, 1986.
27 D. J. Rose, Jr., and J. W. Jorgenson, *Anal. Chem.*, 60 (1988) 642.
28 J. C. Giddings, *Dynamics of Chromatography, Part I, Principles and Theory*, Marcel Dekker, New York, 1965, Ch. 2.
29 C. E. Evans and V. L. McGuffin, *Anal. Chem.*, 60 (1988) 573.
30 B. L. Karger, L. R. Snyder and C. Horvath (Editors), *An Introduction to Separation Science*, Wiley, New York, 1973, Ch. 5.
31 E. L. Johnson and R. Stevenson, *Basic Liquid Chromatography*, Varian Associates, Palo Alto, CA, 1978, Ch. 9.
32 B. A. Bidlingmeyer and F. V. Warren, Jr., *Anal. Chem.*, 56 (1984) 1583A.